

**USING *NEW HORIZONS* OBSERVATIONS OF PLUTO AS A BOOTSTRAP TO DERIVE COMPOSITION MAPS OF TRITON.** J. C. Cook<sup>1</sup>, A. Emran<sup>2</sup>, <sup>1</sup>Pinhead Institute, Telluride, CO., <sup>2</sup>NASA JPL, California Institute of Technology, Pasadena, CA, (jasoncampbellcook@gmail.com)

**Motivation:** At the time of *Voyager 2*'s encounter with Triton, ground-based observations had identified CH<sub>4</sub> and N<sub>2</sub>-ices on its surface [1, 2, 3]. Since then, CO, CO<sub>2</sub>, H<sub>2</sub>O, and HCN have also been identified [4, 5, 6]. On Pluto, N<sub>2</sub>, CH<sub>4</sub>, CO, and H<sub>2</sub>O-ices have also been identified [7, 8, 9]. The distribution and physical parameters (i.e., mass fraction, grain size) across Pluto's surface at the scale of a few km/pix have been mapped by applying Hapke theory to *New Horizons* spectral data [10, 11, 12]. *Voyager 2*, however, could not obtain near-infrared spectral information similar to *New Horizons*, thus limiting our understanding of the distribution of ices across Triton's surface. Even using the best Earth-based observatories (i.e., Keck's OSIRIS), we can only resolve Triton by several pixels, yielding spatial resolutions of a few hundred km/pix. The *James Webb Space Telescope (JWST)* will improve spectral sensitivity and range, but not spatial resolution. *Voyager 2*, however, did provide a detailed view of Triton with images ranging from the near-ultraviolet to visible spectral range (280 to 650 nm). The *Voyager 2*/ISS violet and blue filters overlap with the *New Horizons*/MVIC blue filter, and the *Voyager 2*/ISS green and orange filters overlap with the *New Horizons*/MVIC red filter. We illustrate how the *Voyager 2*/ISS filters overlap with *New Horizons*/MVIC filters in Fig. 1. *Voyager 2*/ISS lacked a filter similar to the *New Horizons*/MVIC NIR filter. ISS and MVIC both carried narrow-band CH<sub>4</sub> filters but were centered at different wavelengths. In the case of ISS, the CH<sub>4</sub> filter favored the detection of gaseous CH<sub>4</sub> in the atmospheres of the giant planets, not solid CH<sub>4</sub> on Triton. Around the same time as the encounter, ground-based observers obtained near-infrared disk-integrated spectra of Triton's encounter hemisphere, thus providing a contemporaneous record of Triton's disk-integrated near-infrared spectrum at the time of the encounter.

**Observations:** We identified five sets of images of Triton from *Voyager 2*/ISS in the PDS/OPUS3 archives. These images cover all the ISS broadband filters (UV, violet, blue, green, and orange) using narrow and wide-angle cameras. The data are calibrated (in units of  $I/F$ ) and geometrically corrected.

We compare *Voyager 2* color observations of Triton with *New Horizons*/Ralph observations of Pluto. Ralph is a dual channel instrument with MVIC (Multi-spectral Visible Imaging Camera), the visible color imager, and LEISA (Linear Etalon Imaging Spectral Array), the near-infrared spectrograph. MVIC images the surface in blue (0.40-0.55  $\mu\text{m}$ ), red (0.54-0.70  $\mu\text{m}$ ), near-

Table 1: Table of observations.

Filters used	Distance (km)	Resolution (km/pix)
Triton/ISS – narrow field camera		
UV, V, B, G, O	2,510,000	20.8
UV, V, B, G, O	2,110,000	17.4
UV, V, B, G, O	1,150,000	9.0
UV, V, B, G, O	540,000	4.1
Triton/ISS – wide field camera		
V, B, G, O, CH <sub>4</sub> -U	150,000	9.0
Pluto/Ralph		
instrument mode	Distance (km)	Resolution (km/pix)
LEISA	114,000	6-7
LEISA	103,000	6-7
MVIC	34,000	0.66

infrared (0.78-0.98  $\mu\text{m}$ ), a narrow CH<sub>4</sub>-band (0.86-0.91  $\mu\text{m}$ ), and panchromatic (0.40-0.98  $\mu\text{m}$ ) wavelength regions[13]. LEISA covers the spectral range from 1.25 to 2.50  $\mu\text{m}$  at a resolving power ( $\lambda/\Delta\lambda$ ) of 240 and 2.10 to 2.25  $\mu\text{m}$  at a resolving power of 560. The Triton and Pluto observations for this work are listed in Table 1.

**Procedure:** Previous studies of Triton using the ISS observations have grouped the ISS data by terrain type [14, 15, 16]. For the following discussion, we follow the formalism by [14] where six terrain types were identified. For this abstract, we present example spectra from four individual points on Triton from units 1, 2, 5, and 6. These spectra are shown as the points in Figs 1-4. Unit 1 corresponds to the dark northern equatorial band, unit 2 corresponds to the dark patches around the south polar cap, unit 5 is the south polar cap, and unit 6 is the bright fringe along the margin of the south polar cap.

To link the *Voyager 2* data to *New Horizons*, we fit the ISS data to a spectral reflectance model following Hapke theory [17, 18]. Our models assume a simple composition of Triton tholins[19] and H<sub>2</sub>O-ice[20] mixed at the granular level. The solid lines in Figs 1-4 show the modeled spectrum over the ISS spectral range and interpolated outward to cover the MVIC filter ranges. At the meeting, we will present images of Triton as if viewed with MVIC. We will perform a clustering analysis of the Triton data. And we will also show preliminary compositional maps of Triton derived from this work.

**Acknowledgements:** The authors acknowledge the support of the NASA ROSES NFDAP (NNH18ZDA001N) program.

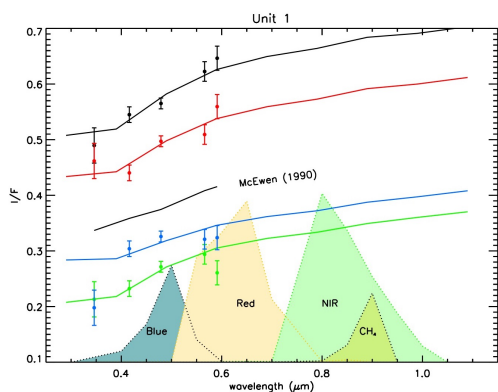


Figure 1: Spectra (points) and Hapke model (lines) from four random points in Unit 1, the dark northern equatorial band. Also shown are the filter band passes corresponding to *New Horizons*/MVIC.

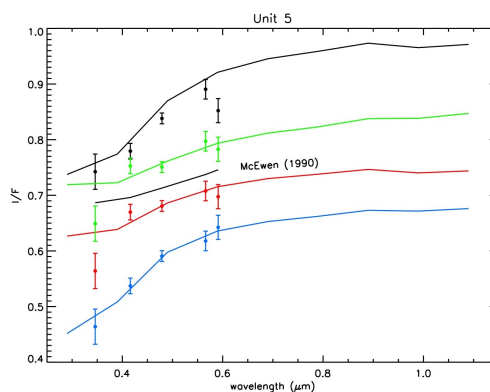


Figure 3: Spectra (points) and Hapke model (lines) from four random points in Unit 5, the south polar cap.

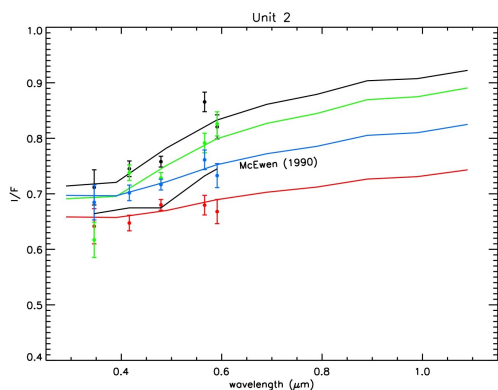


Figure 2: Spectra (points) and Hapke model (lines) from four random points in Unit 2, dark patches around the south polar cap.

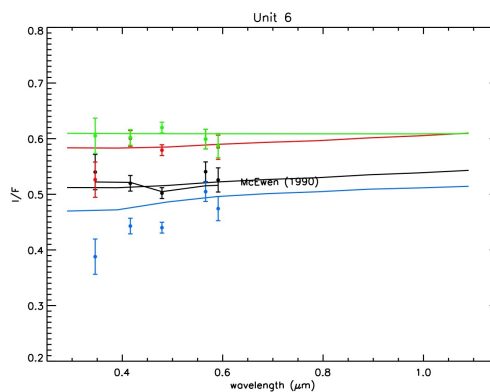


Figure 4: Spectra (points) and Hapke model (lines) from four random points in Unit 6, the bright fringe along the margin of the south polar cap.

**References:** [1] Cruikshank, D. P., et al. (1979) *ApJ* 233(3):1016. [2] Cruikshank, D. P., et al. (1984) *Icarus* 58:293. [3] Cruikshank, D. P., et al. (1984) *Icarus* 58(2):306. [4] Cruikshank, D. P., et al. (1993) *Science* 261:742. [5] Cruikshank, D. P., et al. (2000) *Icarus* 147:309. [6] Burgdorf, M., et al. (2010) *ApJL* 718(2):L53. [7] Cruikshank, D. P., et al. (1976) *Science* 194:835. [8] Owen, T. C., et al. (1993) *Science* 261:745. [9] Grundy, W. M., et al. (2016) *Science* 351:aad9189. [arXiv:1604.05368](https://arxiv.org/abs/1604.05368). [10] Protopapa, S., et al. (2017) *Icarus* 287:218. [arXiv:1604.08468](https://arxiv.org/abs/1604.08468). [11] Schmitt, B., et al. (2017)

*Icarus* 287:229. [12] Cook, J. C., et al. (2019) *Icarus* 331:148. [13] Reuter, D. C., et al. (2008) *Space Sci. Rev.* 140:129. [arXiv:0709.4281](https://arxiv.org/abs/0709.4281). [14] McEwen, A. S. (1990) *Geophys. Res. Lett.* 17(10):1765. [15] Hillier, J., et al. (1991) *J. Geophys. Res.* 96:19211. [16] Hillier, J., et al. (1994) *Icarus* 109(2):296. [17] Hapke, B. (1993) *Theory of reflectance and emittance spectroscopy*. [18] Hapke, B. (2012) *Theory of Reflectance and Emittance Spectroscopy*. [19] Khare, B. N., et al. (1994) vol. 26 of *Bulletin of the American Astronomical Society* 1176. [20] Warren, S. G. (1984) *Applied Optics* 23:1206.